



Original scientific paper

## Effect of sintering temperature and time on corrosion characteristics of aluminum matrix composites

Sahib M. Mahdi and Lubna Ghalib✉

Materials Engineering Department, Mustansiriyah University, Bab Al-Muadham 46049, Baghdad-Iraq

Corresponding author: ✉ [lubnaghalib81@uomustansiriyah.edu.iq](mailto:lubnaghalib81@uomustansiriyah.edu.iq)

Received: May 15, 2023; Accepted: July 21, 2023; Published: July 26, 2023

### Abstract

Aluminum matrix composites outperform traditional alloys in terms of mechanical properties and corrosion resistance. Silicon carbide is the main reinforcing material in aluminum-based composites that have developed rapidly in recent years. In this investigation, aluminum-silicon carbide composites were prepared through powder metallurgy with 10 and 20 wt.% of silicon carbide reinforcement. The influence of the SiC content, sintering temperature, and sintering time on the corrosion behavior of prepared Al-SiC composites in 0.5 M hydrochloride acid solution was assessed. The surface microstructure was characterized by scanning electron microscopy with energy dispersive analysis and X-rays. The experimental results demonstrated how the sintering parameters can affect the corrosion characteristics of sintered samples. The electrochemical analysis curves showed that when increasing the sintering temperature and sintering time, there is a possibility of self-repair of damaged passive film on the surface while further reinforcing of the composite with silicon carbide prevents penetration of chloride ions. The SEM images and EDS analysis of composite surfaces after being corroded in 0.5 M HCl revealed that increasing the sintering temperature and prolonging the sintering time reduce the pitting corrosion of composites.

### Keywords

Aluminum-based composite; silicon carbide; powder metallurgy; sintering parameters

### Introduction

The demand for composite materials has become essential for modern technologies because of already-reached improvements in their physical and mechanical properties. Recently, metal matrix composites (MMC), *i.e.*, metals reinforced with some fibers or particles, have also been advanced. Aluminum matrix composites have lightweight properties, high environmental resistance, high specific strength and stiffness, good wear resistance, high thermal and electrical conductivity, low density, high toughness, and high corrosion resistance. These excellent properties encourage further research and development for further improvement of properties in order to extend their

applications [1-5]. Currently, aluminum matrix composites have extensive applications in the aerospace, military, and car industries [6,7].

Ceramic particles are the most commonly employed materials for reinforcing aluminum matrices like SiC, Si<sub>3</sub>N<sub>4</sub> [8], Al<sub>2</sub>O<sub>3</sub>, and TiC [9]. Al-SiC composites have lately received a lot of interest [10]. Silicon carbide (SiC) remains one of the most commonly used reinforcements in the production of aluminum-based composites due to its excellent resistance to acids and alkalis. The dispersion of SiC substituents inside the matrix materials is influenced by several characteristics, including the molten matrix flow and deformation, the technique of incorporation grains, and their interaction throughout the admixture process [11]. The main disadvantage of Al-SiC is that it is highly susceptible to corrosion due to the influence of intermetallic compounds on the resistance of aluminum matrix to surface degradation. The defects in the protective aluminum oxide film, discontinuities, inclusions, and increased regions of corrosion may be due to the reinforcement of SiC. The resulting microstructural heterogeneity makes Al-SiC more susceptible to corrosion due to interfacial problems and galvanic impact [12].

Processing parameters have a considerable effect on the composite microstructure and as a result, on its corrosion behavior [11,13]. The differences in sintering parameters of Al-SiC can directly affect its microstructure and properties. Previous research on the modification of sintering parameters in the metal matrix composite fabrication process led to improved corrosion resistance. Guo *et al.* [14] examined the effect of sintering temperature on the corrosion behavior of Ti-24Nb-4Zr-7.9Sn alloy made by powder metallurgy and found that alloys sintered at higher temperatures have excellent corrosion resistance due to increased density and decreased porosity. In contrast, alloys sintered at low temperatures have poor corrosion resistance due to decreased density and porosity. Gupa *et al.* [15] evaluated the effect of sintering parameters on the corrosion resistance of Fe-Al<sub>2</sub>O<sub>3</sub> matrix composite fabricated by powder metallurgy. The authors found that the effect of acid attack was more intense for the sample sintered at a lower temperature and for a shorter time than for the sample sintered at a higher temperature and for a longer time. Veerappan *et al.* [16] investigated the impact of the sintering temperature and SiC content varied from 0 to 12 wt.% on the mechanical characteristics and corrosion resistance of Ni-Co-Cr-SiC composites. It was found that the mechanical characteristics and corrosion resistance of Ni-Co-Cr-SiC composites were improved by increasing the sintering temperature and SiC content. Azaath *et al.* [17] investigated the effect of silicon carbide and sintering temperature on the results of compression and hardness tests, microstructure, and corrosion behavior of the Cu-20Al-4Ni composite synthesized by the powder metallurgy route. They found that the corrosion resistance of composites sintered at higher temperatures was greater than that of composites sintered at lower temperatures. It was concluded that both the sintering temperature and SiC reinforcement improve corrosion resistance.

From the literature survey, it was found that the sintering process parameters of metal matrix composites sintered by powder metallurgy have a significant effect on corrosion resistance. Corrosion resistance is a very important parameter in determining the potential use of these materials. Reinforced SiC in the aluminum matrix improves the mechanical properties of composites, but corrosion resistance depends on the fabrication conditions [18]. To our knowledge, there is no publication on the effect of sintering parameters on the corrosion resistance of aluminum composites reinforced with SiC particles. In the present work, the effects of sintering temperature and sintering time on the corrosion properties of Al-SiC metal matrix composites synthesized by powder metallurgy techniques are experimentally investigated.

## Experimental

The matrix material was aluminum (Al) powder of purity 99.5 %, while the reinforcement was silicon carbide. The powders were precisely weighed to obtain the proper stoichiometric composition of Al-10SiC and Al-20SiC. The powder was combined in a tube according to the specified weight ratio using an electric parallel mixer for two hours at 70 rpm. Double-action tool steel dies with a diameter of 11 mm and a height of 30 mm were used to compress the composite powder, which was pressed under a pressure of 146 MPa.

Figure 1 depicts a highly vacuumed tubular furnace where the compacts were sintered at 500 and 550 °C for 2 and 3 hours, respectively. Cylindrical shapes of sintered samples were removed from the vacuum atmosphere tube furnace, as illustrated in Figure 2, and allowed to cool to room temperature.



**Figure 1.** Vacuumed furnace system



**Figure 2.** Sintered Al-10SiC and Al-20SiC composites

The composite sample was cold-mounted in an epoxy resin, following a similar procedure described elsewhere [19]. The exposed flat surface of the mounted part was polished using emery papers of different grades, from 320 to 1000 grits. The corrosion studies were performed at room temperature using a Gamry electrochemical cell with three electrodes connected to a Gamry instrument potentiostat/galvanostat with a Gamry framework system. A saturated calomel electrode (SCE) was used as a reference electrode, a platinum electrode as an auxiliary electrode, and Al-SiC samples as working electrodes with a cross-sectional area of 0.95 cm<sup>2</sup> exposed to the solution. The measurements of potentiodynamic polarization were performed by dipping the working electrode in 0.5 M HCl solution for 1000 s to ensure steady-state condition. The potential was scanned at a scan rate of 2.5 mV s<sup>-1</sup> from -0.25 to +0.25 V vs. SCE.

Phase analysis of corroded surfaces after the electrochemical experiment in 0.5 M HCl solution was examined by recording X-ray diffraction (XRD) patterns. Energy dispersive spectroscopy (EDS) was used for targeted analysis of the sample surface. Scanning electron microscopy (SEM) provided a characterization of the morphology of corroded surfaces.

## Results and discussion

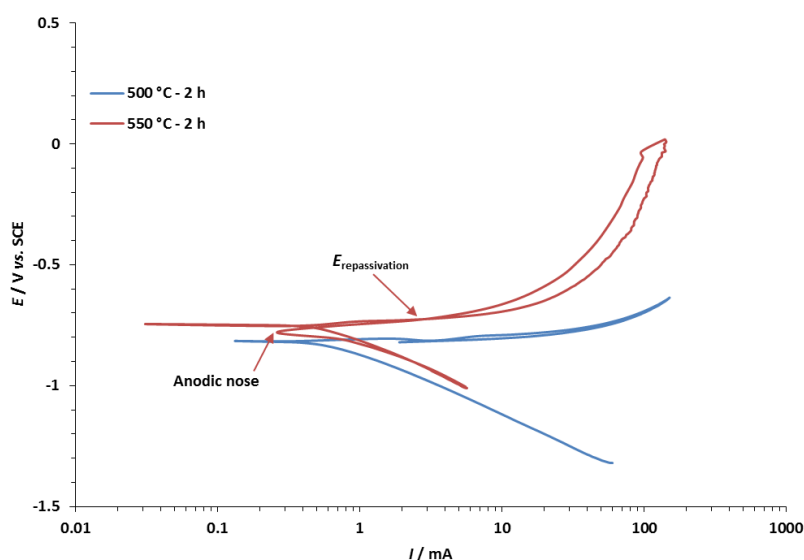
### *Cyclic potentiodynamic polarization measurements*

Cyclic potentiodynamic polarization experiments were performed to report corrosion parameters determined by evaluating the influence of sintering temperature and sintering time on corrosion properties of Al-SiC composite in 0.5 M hydrochloric acid solution. It is essential to consider both the sintering temperature and the sintering time. Higher sintering temperatures can

result in faster densification with less sintering time, but the coarsening rate will rise. When the sintering temperature is lower, the sintering time must be extended to allow diffusion and densification [20]. Grain growth may be possible with a longer sintering time [21]. The main controlling factor in the sintering process is the sintering temperature [22].

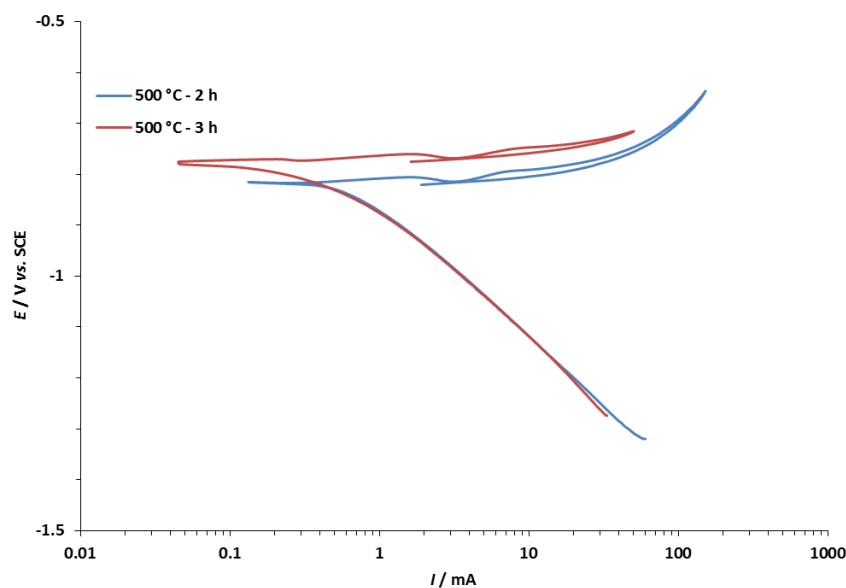
Figures 3 and 4 show cyclic potentiodynamic polarization curves of Al-10SiC composites sintered at different temperatures and times and exposed to 0.5 M HCl solutions at room temperature (~25 °C). Figure 3 illustrates the influence of sintering temperature on the cyclic potentiodynamic curve for a 10 wt.% SiC composite. The composites were sintered at 500 and 550 °C with a fixed sintering time of 2 hours. The cyclic polarization curve for the composite sintered at 500 °C for 2 hours shows an active dissolution in the anodic branch with no transition to passivation. An incomplete positive hysteresis loop with a higher current in the reverse scan than the forward scan resulted from reversing the potential in the backward direction. This pointed toward the inability of the oxide passive film to re-passivate or cause pit initiation in 0.5 M HCl solution. This observation agrees with the study of Loto and Solomon [23], who observed a deterioration of passive film and its inability to self-repair due to the significant effect of chloride concentration on the pitting corrosion of aluminum.

Increasing the sintering temperature to 550 °C remarkably reduced the values of anodic current to develop an oxide film, which is indicated by the large passive region, while the cathodic current has only slightly increased. Moreover, the corrosion potential value was shifted to a more positive direction, with no indication of pitting corrosion. The more positive corrosion potential value is an indication of higher corrosion resistance under testing conditions, as reported by Guo *et al.* [14]. This proves that increasing the sintering temperature greatly decreases the extent of uniform corrosion. There is a complete negative hysteresis loop, with a current in the reverse scan being lower than the current in the forward scan, and an anodic nose also exists. The initiation of pitting corrosion and re-passivation of the composite has been suggested to occur at a higher sintering temperature. The area of the hysteresis loop also increased with increasing the sintering temperature, demonstrating that the greater the disruption of the passive film, the more difficult it is to restore, as Esmailzadeh *et al.* [24] reported. The repassivation potential ( $E_{rp}$ ) of Al-10SiC sintered at 550 °C for 2 hours is -705.1 mV, *i.e.*, nobler than the corrosion potential of composite, which means that no pitting corrosion exists at the potential between them.



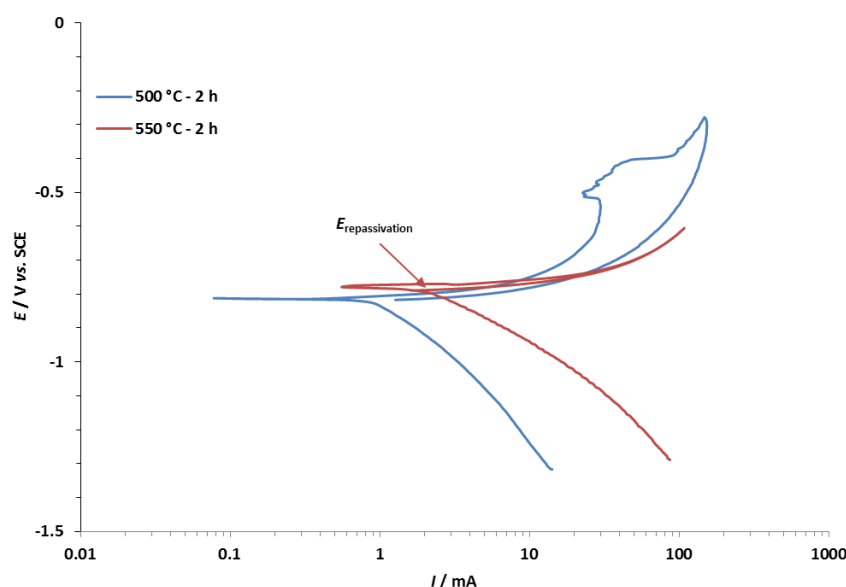
**Figure 3.** Cyclic potentiodynamic polarization curves (0.5 M HCl,  $2.5 \text{ mV s}^{-1}$ ) for 10 wt.% SiC composite sintered at 500 and 550 °C for 2 hours

Figure 4 presents cyclic potentiodynamic polarization curves of 10 wt.% SiC sintered at 500 °C for 2 and 3 hours in 0.5 M HCl solution. It is observed from Figure 4 that both composites displayed relatively similar polarization trends with increasing potential, except for a small difference in the anodic branch. From the cyclic polarization curve, it can be observed that the hysteresis loop for both curves was positive and incomplete, which confirmed that there was no pitting corrosion and indicated that the oxide passive film is unable to re-passivate in 0.5 M HCl solution.



**Figure 4.** Cyclic potentiodynamic polarization curves ( $0.5\text{ M HCl}$ ,  $2.5\text{ mV s}^{-1}$ ) for 10 wt.% SiC composite sintered at 500 °C for 2 and 3 hours

The cyclic potentiodynamic results obtained for 20 wt.% SiC composites sintered at 500 and 550 °C for 2 hours are presented in Figure 5. Both cyclic polarization curves display positive hysteresis as the sintering temperature increases, revealing the breakdown of the passive film.



**Figure 5.** Cyclic potentiodynamic polarization curves ( $0.5\text{ M HCl}$ ,  $2.5\text{ mV s}^{-1}$ ) for 20 wt.% SiC composite sintered at 500 °C and 550 °C for 2 hours

However, the sample at 550 °C crossed the anodic arm at a protection potential of -787.0 mV, as anticipated, indicating the tendency of the oxide passive film to re-passivate and pit initiation. The size

of the hysteresis loop decreases when the sintering temperature of the samples is raised, which again is in agreement with Esmailzadeh *et al.* [24]. The smaller the hysteresis loop, the less disruption of the passive film possible to restore. When increasing the sintering temperature from 500 to 550 °C, the cathodic branch shifts towards a higher current, indicating that the cathodic reaction is increased by the addition of SiC reinforcement at a higher sintering temperature.

Figure 6 depicts the cyclic potentiodynamic curves of 20 wt.% SiC composites sintered at 500 °C for 2 and 3 hours. The curves in Figure 6 indicate shifts of both cathodic and anodic branches toward lower current values when increasing the sintering time from 2 to 3 hours. This means the sample with increasing SiC content, prepared at a higher sintering time, shows less corrosion current. This is due to the good dispersion of SiC particles in the Al matrix at this sintering temperature compared to samples at a lower sintering time. The hysteresis loop of Al-20SiC composite sintered at 500 °C for 2 hours is positive and incomplete when compared to the composite sintered for 3 hours, which is positive and complete, with the repassivation potential  $E_{rp} = -775.8$  mV vs. SCE. The value of repassivation potential is nobler than corrosion potential, indicating the stoppage of propagation pits and the formation of a stable oxide film.

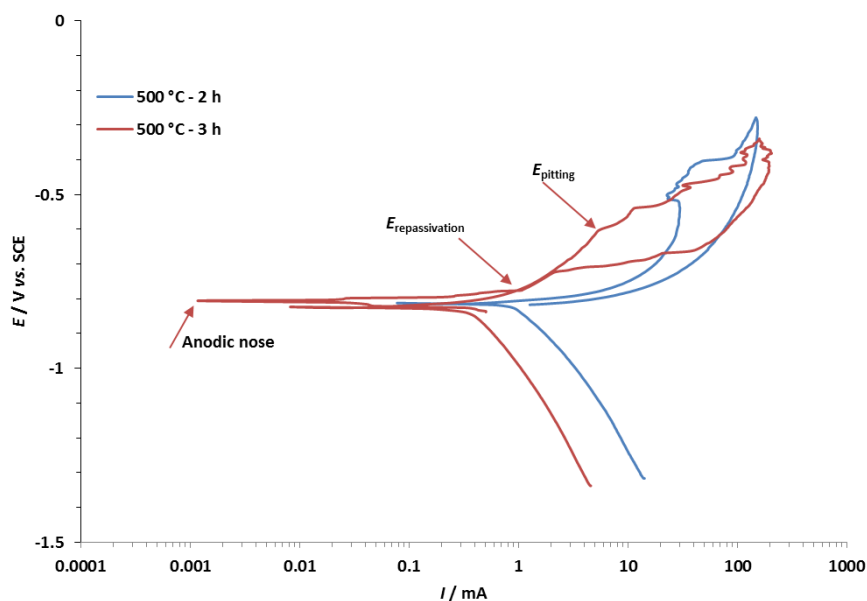


**Figure 6.** Cyclic potentiodynamic polarization curves ( $0.5$  M HCl,  $2.5$  mV s<sup>-1</sup>) for 20 wt.% SiC composite sintered at 500 °C for 2 and 3 hours

Table 1 presents corrosion parameter values determined from potentiodynamic polarization curves (Figures 3-6), including the values of cathodic Tafel slope ( $\beta_c$ ), anodic Tafel slope ( $\beta_a$ ), corrosion potential ( $E_{corr}$ ), corrosion current ( $I_{corr}$ ), and corrosion rate (CR). The corrosion rate was calculated using the following equation:

$$CR = \frac{0.00327 E_w J_{corr}}{DA} \tag{1}$$

where CR is corrosion rate (mm year<sup>-1</sup>),  $E_w$  is the equivalent weight of composite,  $I_{corr}$  is corrosion current obtained from Tafel slope ( $\mu$ A),  $D$  is the density of composite (g cm<sup>-3</sup>),  $A$  is electrode area (cm<sup>2</sup>). Here, the composite density was calculated based on the weight content and density of both compounds (Al and SiC) in the composite.

The corrosion results listed in Table 1 clearly show that aluminum matrix composite with 90 wt.% of aluminum displays higher resistance to pitting corrosion due to the strong protective oxide formation. However, the presence of SiC improves the strength of the composite, but it also leads

to the development of intermetallic particles, second phases, and precipitates, which inevitably incorporate micro-galvanic cells throughout the composite surface.

**Table 1.** Corrosion parameters determined from polarization curves for Al-SiC composites in 0.5 M HCl

Sample	Sintering conditions	$\beta_a / \text{mV decade}^{-1}$	$\beta_c \text{ mV / decade}^{-1}$	$I_{\text{corr}} / \mu\text{A}$	$E_{\text{corr}} / \text{mV}$	CR, mm year <sup>-1</sup>
Al-10SiC	500 °C (2 h)	17.10	221.5	534.0	-814.0	8.66
	500 °C (3 h)	17.50	132.9	164.0	-777.0	2.57
	550 °C (2 h)	29.80	218.5	472.0	-744.0	7.67
Al-20SiC	500 °C (2 h)	47.50	403.0	1100	-811.0	17.92
	500 °C (3 h)	152.1	724.0	645.0	-823.0	10.47
	550 °C (2 h)	23.00	237.6	2.050	-777.0	32.33

### X-ray diffraction analysis

The X-ray diffraction (XRD) patterns of Al-20SiC composites processed by powder metallurgy after corrosion in 0.5 M HCl solution are illustrated in Figure 7. For Al-20SiC composite samples fabricated at different sintering temperatures and times, four high-intensity peaks and many low-intensity peaks are displayed in XRD spectra. Aluminium phases are shown by four strong diffraction peaks at  $2\theta$  values of 38.45, 44.71, 65.09, and 78.23°, while low-intensity peaks correspond to SiC and intermetallic compounds formation during sintering. These peaks can be used to prove their presence in fabricated aluminum-metal composites. Generally, Figure 7 shows XRD patterns of composites that are similar to each other and are dominated by the aluminum and SiC peaks. The small oxide peaks were seen in the XRD analysis of Al-SiC composites sintered at 500 and 550 °C for 2 and 3 hours, indicating Al<sub>2</sub>O<sub>3</sub> formation on the surface.

There is not much change in the shift of peaks related to Al and SiC, but the intensity of peaks increases while increasing the sintering temperature gradually. It is found that the intensity of Al is higher in the composite sintered at 550 °C in comparison to the composite sintered at 500 °C for the same sintering time. The reason for this is due to the high temperature of diffusion. The porosity of the composite was expected to decrease significantly when the sintering temperature was increased and the contact among the powder particles was enhanced, which ultimately increased densification.

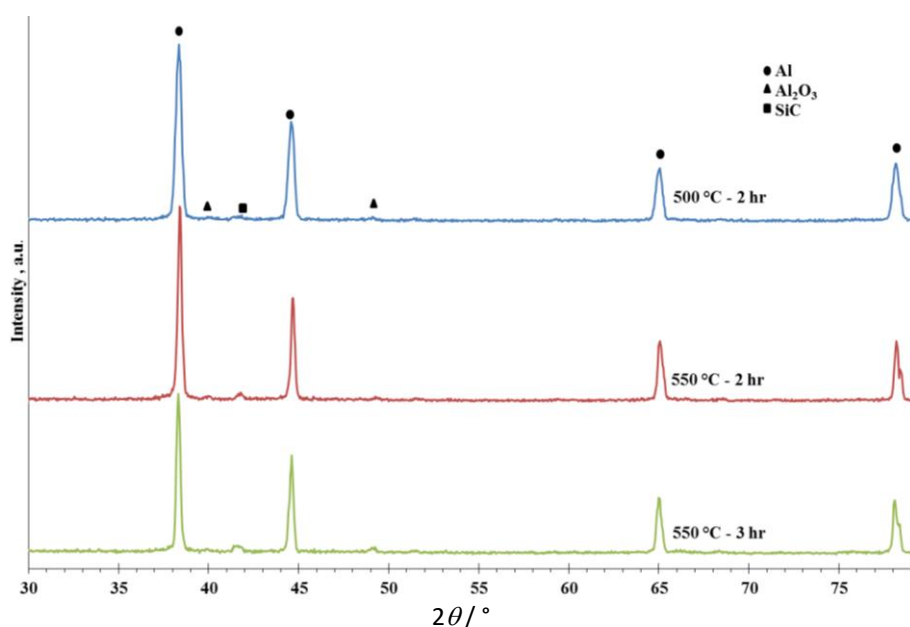
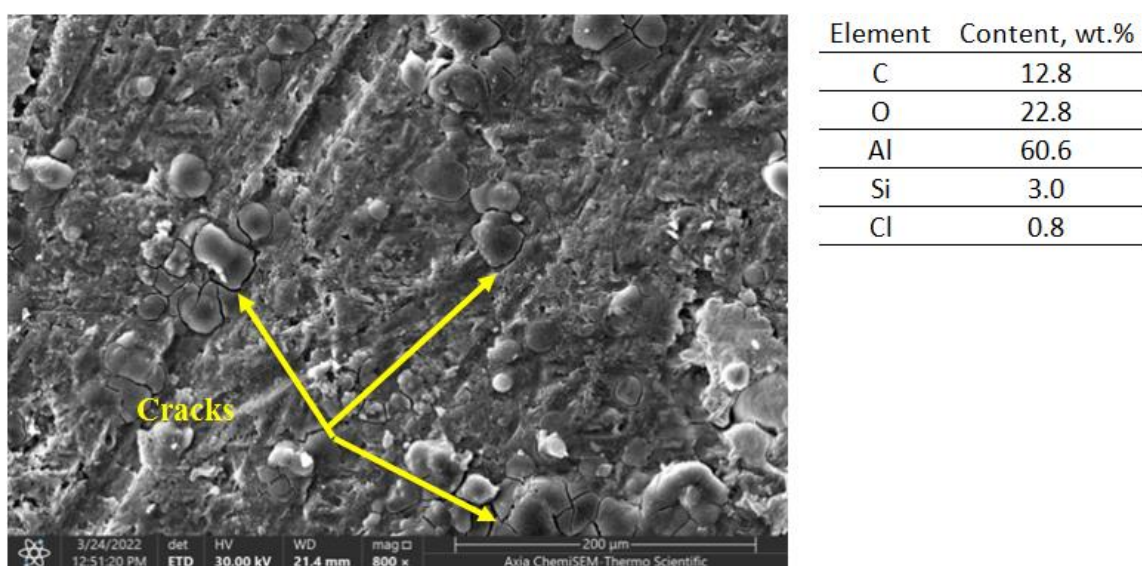


**Figure 7.** XRD patterns of sample with 20 wt.% SiC at different sintering conditions after exposure to 0.5 M HCl solution

### Scanning electron microscopy analysis

Scanning electron microscopy analysis was conducted to determine if pitting corrosion occurs after electrochemical testing and to determine the influence of sintering temperature and sintering time on the surface morphology of composites sintered at 500 and 550 °C for 2 and 3 hours, respectively. The presence, morphology, and distribution of components on the corroded surface were examined using scanning electron microscopy and energy dispersive spectroscopy, as shown in Figures 8-11.

Figure 8 shows the surface morphology of Al- 20SiC composite sintered at 500 °C for 2 hours after corrosion in 0.5 M HCl solution. The microstructure shows the presence of numerous cracks formed in the passive oxide layer, which correspond to trans-passivation as well as the presence of some small pores due to the attack of the aggressive chloride solution. The elemental analysis revealed that the film on the composite contains significant amounts of oxygen and aluminum, which confirms the formation of aluminum oxide film on the surface of a composite, but this film contains a large number of cracks. According to the EDS analysis, the presence of the high amount of silicon on the surface of the composite indicates that the silicon carbide grains were not completely covered by the oxide film, which helps to minimize porosity in the composite, as was investigated by Pech-Canul and Makhlof [25].



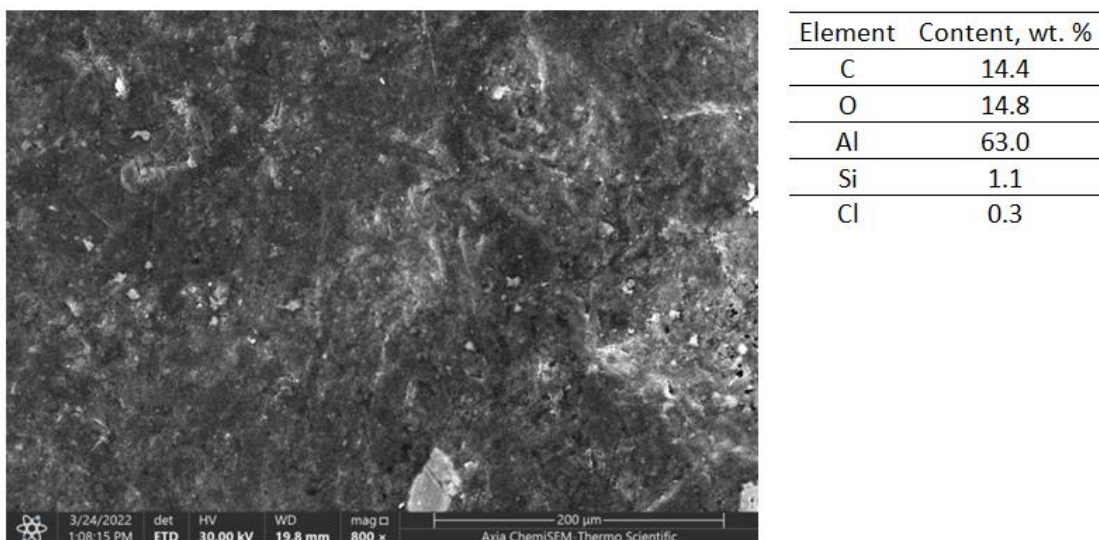
**Figure 8.** SEM micrograph and EDS analysis of 20 wt.% SiC composite sintered at 500 °C for 2 hours after exposure to 0.5 M HCl

Figure 9 demonstrates the development of microstructure with the rise of the sintering temperature. It is seen that with increasing sintering temperature, a stable passive layer of aluminum oxide is formed, which is more homogeneous in thickness and free of cracks due to higher diffusion rates. This was clearly confirmed by the polarization curve behavior with repassivation potential in Figure 5. The increased sintering temperature causes a slight reduction in the oxygen content of the composite, which was identified by selected field EDS analysis, while the content of aluminum is high. This means the formed alumina layer continues on the surface, increasing the corrosion rate. A similar observation was discussed in a recent study by Aruna and Arivukkarasan [26].

From SEM examination in Figures 8 and 9, the sample sintered at 550 °C improves the homogeneous distribution of reinforcement particles and reduces pore formation considerably. This can be explained by the fact that when the sintering temperature rises, high atom diffusion occurs, which leads to a reduction in the pores and the possibility of the oxide film re-passivation. Previous



work by Rahimian *et al.* [6] found that samples had greater strength against acid attacks when the bonding strength between the particles increased with rising sintering temperatures.



**Figure 9.** SEM micrograph and EDS analysis of 20 wt.% SiC composite sintered at 550 °C for 2 hours after exposure to 0.5 M HCl

Figure 10 shows the morphology of the specimen of 20 wt.% SiC sintered at 550 °C for 3 hours after the corrosion test. EDS analysis at 550 °C for 3 hours showed a decrease in the amount of aluminum to around 38.1 wt.% with a high content of oxygen in the corrosion products, demonstrating the formation of a thick oxide film over the composite surface. The formation of a stable oxide film on the composite surface helps to reduce the corrosion rate, as shown in Table 1.

After all, it can be concluded that the specimen of 20 wt.% SiC sintered at 550 °C for 3 hours has significantly improved corrosion resistance due to the complete reaction and the optimum amount of aluminum oxide formed. Increasing the sintering time from 2 to 3 hours has a slight effect on the corrosion rate. This might indicate that the disappearance of the small-sized porosity is affected by increasing the sintering time, but higher sintering temperatures are also required to significantly reduce the size of the large pores, which enhances corrosion resistance and prevents the formation of pits.

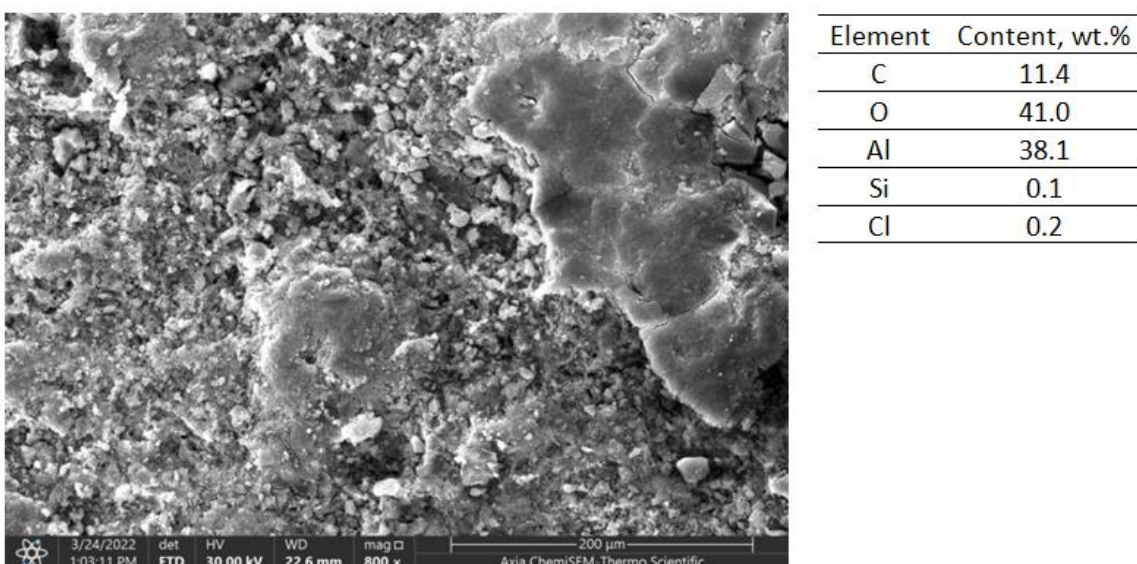
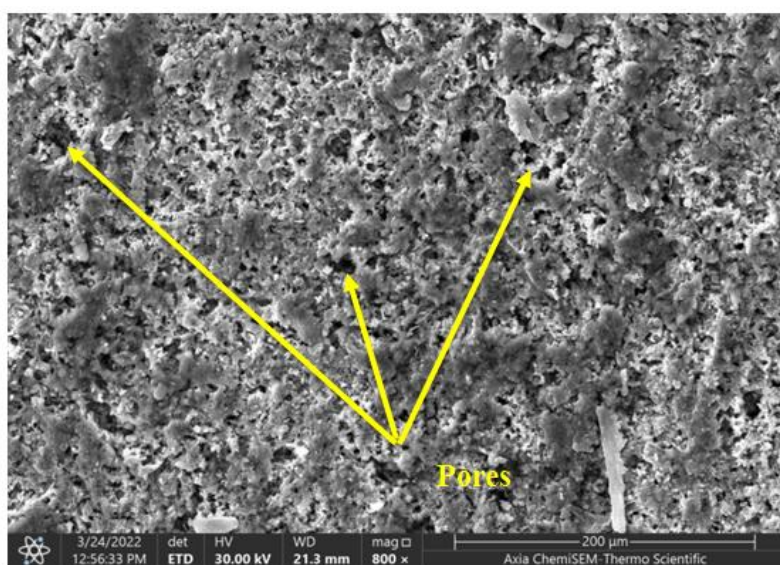


**Figure 10.** SEM micrograph and EDS analysis of 20 wt.% SiC composite sintered at 550 °C for 3 hours after exposure to 0.5 M HCl

Figure 11 shows the SEM image and EDS analysis of Al-10SiC composite sintered at 550 °C for 2 hours. A wide spread of SiC in the Al matrix along with micropores indicates severe pitting corrosion. This is due to a porous oxide film formed with the possibility of re-passivation. A low amount of oxygen is found during the elemental analysis, which reveals that the surface developed a very thin oxide layer. This is well supported by EDS analysis, which found a high amount of carbon. Despite the fact that a 20 wt.% SiC composite has a higher corrosion rate than a 10 wt.% SiC composite, it is found that increasing sintering temperature and sintering time reduces the number of pits and forms a stable passive film in the same composite.



Element	Content, wt.%
C	26.3
O	8.3
Al	62.1
Si	1.0
Cl	0.2
Fe	0.3
Sb	1.8

**Figure 11.** SEM micrograph and EDS analysis of 10 wt.% SiC composite sintered at 550 °C for 2 hours after exposure to 0.5 M HCl

## Conclusions

The effect of sintering temperature and sintering time on the corrosion behavior of Al-SiC composites fabricated by powder metallurgy and exposed to 0.5 M HCl solution was studied through electrochemical testing and surface analysis techniques. The corrosion behavior was studied for two composites reinforced with a 10 and 20 wt.% content of SiC, sintered at 500 and 550 °C, for 2 and 3 hours, respectively. The effect of sintering temperature was found to be the most significant, followed by the sintering time and SiC content. The highest values of corrosion resistance for Al-SiC composites were obtained at the sintering temperature of 550 °C and a sintering time of 3 hours for both SiC contents (10 and 20 wt.%) in the composites. There is a direct relationship between the formation of pitting corrosion and the sintering temperature and time in a way that increasing the sintering temperature and time enhances the pitting corrosion resistance. XRD analysis revealed the presence of Al with a high peak intensity and SiC with a low peak intensity. A small peak for intermetallic compounds indicates the development of an oxide film on the surface, and this fact was corroborated by EDS analysis. The SEM study of the surface of sintered samples after corrosion in 0.5M HCl revealed that for samples with an increased weight content of SiC content, the corrosion rate increased with the occurrence of pitting corrosion. These corrosion pits, however, were found smaller and shallower for samples sintered at increased temperature and time for both composites.

**Acknowledgement:** The authors would like to thank Mustansiriyah University, Baghdad, Iraq, for its support of the present work.

## References

- [1] E. M. Sharifi, M. H. Enayati, F. Karimzadeh, Fabrication and Characterization of Al-Al<sub>4</sub>C<sub>3</sub> nanocomposite by mechanical alloying, *International Journal of Modern Physics: Conference Series* **05** (2012) 480-487. <https://doi.org/10.1142/S2010194512002371>
- [2] S. M. Mahdi, L. Ghalib, Corrosion Behavior of Al/SiC Composite Prepared by Powder Metallurgy in Chloride Environments, *Journal of Bio-and Tribo-Corrosion* **8** (2022) 8. <https://doi.org/10.1007/s40735-021-00612-6>
- [3] R.A. Kumar, A. Devaraju, A comparative investigation on cast and aging (T6) response on mechanical and dry sliding wear behavior of Al7075/SiC p metal matrix composite, *Surface Review and Letters* **28(6)** (2021) 2150044. <https://doi.org/10.1142/S0218625X2150044X>
- [4] R. A. Kumar, M. Sujithkumar, P. Vikram, S. Arunkumar, S. T. Selvan, G. S. Sharan, A review on tribological behaviour of aluminium metal matrix composites, *AIP Conference Proceedings: Recent trends in Science and Engineering* **2393(1)** (2022) 020006. <https://doi.org/10.1063/5.0079693>
- [5] F. Adel, L. Ghalib, Improving the mechanical properties of glass ionomer cements by incorporation of date seed microparticles, *Emergent Materials* **5** (2023) 1081-1088. <https://doi.org/10.1007/s42247-023-00511-1>
- [6] M. Rahimian, N. Ehsani, N. Parvin, H. R. Baharvandi, The effect of particle size, sintering temperature and sintering time on the properties of Al-Al<sub>2</sub>O<sub>3</sub> composites, made by powder metallurgy, *Journal of Materials Processing Technology* **209(14)** (2009) 5387-5393. <https://doi.org/10.1016/j.jmatprotec.2009.04.007>
- [7] R. A. Kumar, A. Devaraju, Modeling of mechanical properties and high temperature wear behavior of Al7075/SiC/CRS composite using RSM, *Silicon* **13(10)** (2021) 3499-3519. <https://doi.org/10.1007/s12633-020-00801-x>
- [8] R. A. Kumar, B. I. Prasad, C. Bibin, I. J. Thomas, G. Soundararajan, P. R. Darshan, S. Arunkumar, Physical and mechanical characterization of Al7075/Si<sub>3</sub>N<sub>4</sub> metal matrix composite prepared by stir casting technique, *MaterialsToday: Proceedings* **80** (2023) 176-182. <https://doi.org/10.1016/j.matpr.2022.11.096>
- [9] R. A. Kumar, A. Devaraju, S. Arunkumar, Experimental investigation on mechanical behaviour and wear parameters of tic and graphite reinforced aluminium hybrid composites, *MaterialsToday: Proceedings* **5(6)** (2018) 14244-14251. <https://doi.org/10.1016/j.matpr.2018.03.005>
- [10] A. S. Channi, H. S. Bains, J. S. Grewal, V. S. Chidambanathan, R. Kumar, Tool wear rate during electrical discharge machining for aluminium metal matrix composite prepared by squeeze casting: A prospect as a biomaterial, *Journal of Electrochemical Science and Engineering* **13 (1)** (2023) 149-162. <https://doi.org/10.5599/jese.1391>
- [11] R. T. Loto, P. Babalola, Analysis of SiC grain size variation and NaCl concentration on the corrosion susceptibility of AA1070 aluminium matrix composites, *Cogent Engineering* **5(1)** (2018) 1473002. <https://doi.org/10.1080/23311916.2018.1473002>
- [12] R. A. Kumar, D. Ayyappan, S. Arunkumar, G. Devanand, K. Dasar, N. S. Srivatsav, S. Dhamodharan, A Comprehensive review on fabrication techniques and corrosion behavior on metal matrix composites, *AIP Conference Proceedings: Recent Trends in Science and Engineering* **2393** (2022) 020014. <https://doi.org/10.1063/5.0074274>
- [13] H. A. Abdulghani, L. Ghalib, B. J. Nabhan, Spot Welding Parameters Effect on Surface Corrosion Behavior of Carbon Steel Sheet, *Egyptian Journal of Chemistry* **65(10)** (2022) 531-535. <https://doi.org/10.21608/EJCHEM.2022.117260.5291>
- [14] S. Guo, A. Chu, H. Wu, C. Cai, X. Qu, Effect of sintering processing on microstructure, mechanical properties and corrosion resistance of Ti-24Nb-4Zr-7.9 Sn alloy for biomedical

applications, *Journal of Alloys and Compounds* **597** (2014) 211-216.

<https://doi.org/10.1016/j.jallcom.2014.01.087>

- [15] P. Gupta, D. Kumar, M. Quraishi, O. Parkash, Effect of sintering parameters on the corrosion characteristics of iron-alumina metal matrix nanocomposites, *Journal of Materials and Environmental Science* **6(1)** (2015) 155-167.  
[https://www.imaterenvironsci.com/Document/vol6/vol6\\_N1/19-JMES-1006-2014-Gupta.pdf](https://www.imaterenvironsci.com/Document/vol6/vol6_N1/19-JMES-1006-2014-Gupta.pdf)
- [16] G. Veerappan, M. Ravichandran, M. Meignanamoorthy, V. Mohanavel, Characterization and properties of silicon carbide reinforced Ni-10Co-5Cr (Superalloy) matrix composite produced via powder metallurgy route, *Silicon* **13(4)** (2021) 973-984.  
<https://doi.org/10.1007/s12633-020-00455-9>
- [17] L. M. Azaath, U. Natarajan, G. Veerappan, M. Ravichandran, S. Marichamy, Experimental Investigations on the Mechanical Properties, Microstructure and Corrosion Effect of Cu-20Al-4Ni/SiC Composites Synthesized Using Powder metallurgy Route, *Silicon* **14** (2022) 5993-6002. <https://doi.org/10.1007/s12633-021-01363-2>
- [18] Z. Ahmad, P. Paulette, B. A. Aleem, Mechanism of localized corrosion of aluminum–silicon carbide composites in a chloride containing environment, *Journal of Materials Science* **35** (2000) 2573-2579. <https://doi.org/10.1023/A:1004767113052>
- [19] L. Ghalib, A. K. Muhammad, S. M. Mahdi, Study the effect of adding titanium powder on the corrosion behavior for spot welded low carbon steel sheets, *Journal of Inorganic and Organometallic Polymers and Materials* **31(6)** (2021) 2665-2671.  
<https://doi.org/10.1007/s10904-020-01863-5>
- [20] M. N. Rahaman, *Ceramic Processing and Sintering*, CRC Press, Taylor & Francis Group, Boca Raton, 2017. <https://doi.org/10.1201/9781315274126>
- [21] M. Asadikiya, C. Zhang, C. Rudolf, B. Boesel, A. Agarwal, Y. Zhong, The effect of sintering parameters on spark plasma sintering of B4C, *Ceramics International* **43(14)** (2017) 11182-11188. <https://doi.org/10.1016/j.ceramint.2017.05.167>
- [22] V. V. Vani, S. K. Chak, The effect of process parameters in aluminum metal matrix composites with powder metallurgy, *Manufacturing Review* **5** (2018) 7.  
<https://doi.org/10.1051/mfreview/2018001>
- [23] R. T. Loto, M. M. Solomon, Corrosion resistance and passivation behavior of 3004 AlMnMg and 4044AlSi aluminum alloys in acid-chloride electrolytes, *Materials Research Express* **8(9)** (2021) 096529. <https://doi.org/10.1088/2053-1591/ac286b>
- [24] S. Esmailzadeh, M. Aliofkhazraei, H. Sarlak, Interpretation of cyclic potentiodynamic polarization test results for study of corrosion behavior of metals: a review, *Protection of Metals and Physical Chemistry of Surfaces* **54(5)** (2018) 976-989.  
<https://doi.org/10.1134/S207020511805026X>
- [25] M. Pech-Canul, M. Makhlof, Processing of Al–SiCp metal matrix composites by pressureless infiltration of SiCp preforms, *Journal of Materials Synthesis and Processing* **8** (2000) 35-53. <https://doi.org/10.1023/A:1009421727757>
- [26] M. Aruna, S. Arivukkarasan, Electrochemical behavior of Al-SiC metal matrix composites, *International Journal of Applied Engineering Research* **15(1)** (2020) 1-4.  
[https://www.ripublication.com/ijaer20/ijaerv15n1\\_01.pdf](https://www.ripublication.com/ijaer20/ijaerv15n1_01.pdf)